ACS OMEGA

http://pubs.acs.org/journal/acsodf

Article

Solid Lipid Nanoparticles of Curcumin Designed for Enhanced Bioavailability and Anticancer Efficiency

Sooho Yeo,* Min Je Kim, Young Key Shim, Il Yoon,* and Woo Kyoung Lee*

Cite This: *ACS Omega* 2022, 7, 35875−35884

Read Online

ACCESS | Metrics & More | Article Recommendations | Supporting Information

ABSTRACT: Curcumin (Cur) has anticancer properties but exhibits poor aqueous solubility, permeability, and photostability. In this study, we aimed to develop a solid lipid nanoparticle (SLN) system to enhance Cur bioavailability. The characteristics of Cur-loaded SLNs prepared by sonication were evaluated using UV−vis and Fourier transform infrared spectroscopy. The mean particle size of the stearic acid-based, lauric acid-based, and palmitic acid-based SLNs was 14.70−149.30, 502.83, and 469.53 nm, respectively. The chemical interactions between Cur and lipids involved hydrogen bonding and van der Waals forces. The formulations with high van der Waals forces might produce a neat arrangement between Cur and lipids, leading to a decrease in particle size. The Cur formulations showed enhanced cytotoxicity in HeLa, A549, and CT-26 cells compared with pure Cur. Additionally, the anticancer effect is dependent on particle size and the type of cell line. Therefore, Cur-loaded SLNs have the potential for use in anticancer therapy.

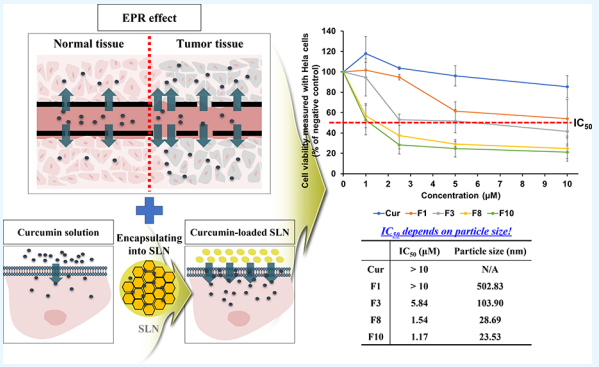

INTRODUCTION

Curcumin (Cur) is an active pharmaceutical ingredient with a wide range of pharmacological effects, including antibacterial, anti-inflammatory (especially beneficial effects on several ocular diseases), antioxidant, and antitumor properties.[1−7] The chemical structure of Cur is diferuloylmethane, which belongs to the polyphenol class.[8−10] The molecular weight of Cur is 368.389 g/mol, and its chemical name is (1E,6E)-1,7-bis(4-hydroxy-3-methoxyphenyl)-1,6-heptadiene-3,5-dione with the chemical formula $C_{21}H_{20}O_6$.[1,4] Cur has been approved as a safe compound by the World Health Organization and US Food and Drug Administration (FDA).[2]

Despite its promising pharmacological effects and safety, the clinical usefulness of Cur in cancer treatment is limited. Cur, a class IV drug of the biopharmaceutical classification system (BCS), is poorly water-soluble, exhibiting a log*P* value of 3.2, and is incompletely absorbed.[11] According to absorption and distribution studies, Cur is absorbed approximately 60% in the gastrointestinal tract and undergoes extensive hepatic first-pass metabolism, which leads to poor bioavailability.[3,12,13] Furthermore, the storage of Cur should be carefully monitored for its photodegradable property.[1] Therefore, it would be advantageous to enhance the aqueous solubility and photostability of Cur to develop more efficient dosage forms.

Various approaches have been reported to overcome these limitations, including structural modification by conjugating water-soluble polymers[14,15] as well as usage of nanoscale drug delivery systems (liposomes,[16] liquid crystals,[17] nano-emulsions,[18] and phospholipid complexes[19]). Specifically, the conventional pharmaceutical strategies in cancer therapy entail a passive targeting based on the enhanced permeation and retention (EPR) effect.[20,21] The formulations loaded with an anticancer drug can increase the drug permeability of blood capillary in targeted tissues compared to when the fluid returns to lymphatic circulation where the particle size is up to 400 nm.[22−24] Hence, alternative drug delivery systems are necessary for cancer therapy.

Solid lipid nanoparticle (SLN) systems appear to be an efficient approach for increasing the aqueous solubility and stability of drugs and decreasing the particle size to the nanoscale level.[8,25−28] In SLN systems, a lipophilic drug is stably dispersed in the water solvent by loading a lipid matrix of SLN via preparing an oil-in-water (O/W) phase.[10,29,30] The solid structure of the SLN system protects an unstable drug from environmental factors such as light, pH, and atmospheric moisture.[31−34] In particular, SLN can be delivered into the lymphatic system upon oral administration by bypassing the liver via forming chylomicrons in enterocytes.[35,36] Thus, drugs embedded in SLNs effectively avoid hepatic first-pass metabolism, enhancing the pharmacological effects of the

Received: July 12, 2022
Accepted: September 8, 2022
Published: September 28, 2022

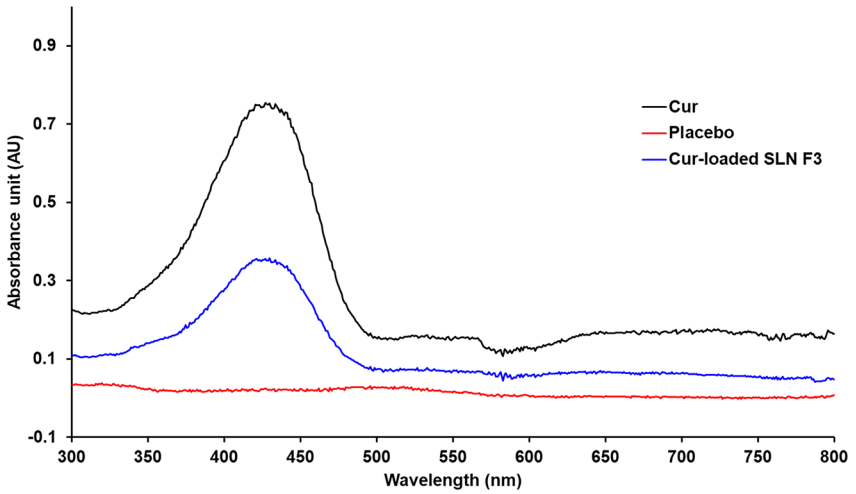

Figure 1. UV−vis spectra for specificity of Cur, placebo, and Cur-loaded SLN F3 (MeOH, 25 °C).

drug.[9,11,35,36] Moreover, this formulation can be used as a brain-targeted drug delivery system when absorbed into the systemic circulation, overcoming one of the most important challenges in pharmaceutical sciences.[37,38] Although the blood−brain barrier, a highly selective semipermeable border, protects the brain parenchyma against circulating toxins or pathogens, it allows the diffusion of hydrophobic molecules.[39]

In the present study, Cur-loaded SLNs were prepared for anticancer treatment using the EPR effect strategy. The characteristics of Cur and Cur-loaded SLNs were evaluated using UV−vis spectroscopy and Fourier transform infrared (FTIR) spectroscopy, along with the evaluation of particle characteristics. The *in vitro* cytotoxic effects of Cur and Cur-loaded SLNs were investigated in three tumor cell lines: HeLa from human cervical cancer, A549 from human lung carcinoma, and CT-26 from mouse colon carcinoma. Additionally, the anticancer effects of Cur on these cell lines were compared and the different mechanisms of Cur were discussed.

RESULTS AND DISCUSSION

Development of an Analytical Method for Cur. Absorption spectra and specificity studies for Cur were carried out to identify the maximum absorption wavelength and to demonstrate the specific absorption spectra. UV−vis spectra showed that the maximum absorption wavelength was 425 nm (Figure 1). The specificity results demonstrated that the placebo SLN (without PS) did not interfere with the analyte. Thus, Cur was analyzed at 425 nm.

Five standard stock solutions of Cur at concentrations ranging from 1 to 20 ppm were used to produce a calibration curve. The correlation coefficient of the calibration curve obtained via linear regression analysis was 0.9998 (Figure S1).

A precision study was conducted to represent the closeness of agreement among measurements from different standard stock solutions with the same concentration. Precision is expressed as the relative standard deviation (RSD) of repeatability. The Cur recovery values were calculated as the RSD% of the absorption unit. The precision results demonstrated that the RSD% value of the Cur recovery was 0.75% (Table S1). This result demonstrates the high precision of the proposed analytical method.

The developed analysis method was tested for its accuracy. Accuracy is defined as the closeness of agreement between the test results and a conventional true or accepted reference value. The accuracy was expressed as the RSD calculated from the Cur recovery. The accuracy results for different concentrations of the standard stock solutions demonstrated that the RSD (%) values of the recovery were 0.26, 0.90, and 0.12% (Table S2), indicating that the developed analytical method has high accuracy.

Preparation and Characterization of Cur-Loaded SLNs. *Preparation Method.* Cur-loaded SLNs were prepared by mixing Cur and various lipids (LA, PA, or SA) and surfactants (PX 188, PX 407, TW 20, or TW 80) via sonication using a modified O/W emulsion method, resulting in various formulations (F1−F11). We also changed amount of lipids and surfactants. The various compositions of Cur-loaded SLNs are summarized in Table 1.

Table 1. Composition of Cur-Loaded SLNs[a]

	drug (mg)	lipid (mg)			surfactant (mg)			
formulation	Cur	LA	PA	SA	PX 188	PX 407	TW 20	TW 80
F1	100	100			200			
F2	100		100		200			
F3	100			100	200			
F4	100			100		200		
F5	100			100			200	
F6	100			100				200
F7	100			100	400			
F8	100			300	200			
F9	100			300	400			
F10	100			500	200			
F11	100			500	400			

[a]Cur, curcumin; LA, lauric acid; PA, palmitic acid; SA, stearic acid; PX 188, Poloxamer 188; PX 407, Poloxamer 407; TW 20, Tween 20; TW 80, Tween 80.

Nanoparticle Size, Polydispersity Index (PDI), and Zeta Potential. Particle characterization studies were conducted to evaluate the effects of various ingredients on the fabrication and concentration of the ingredients. Particle size and PDI parameters are important in cancer therapy because of the passive targeting strategy based on the EPR effect.[20,21] Zeta potential represents the electrical potential on the particle

https://doi.org/10.1021/acsomega.2c04407
ACS Omega 2022, 7, 35875−35884

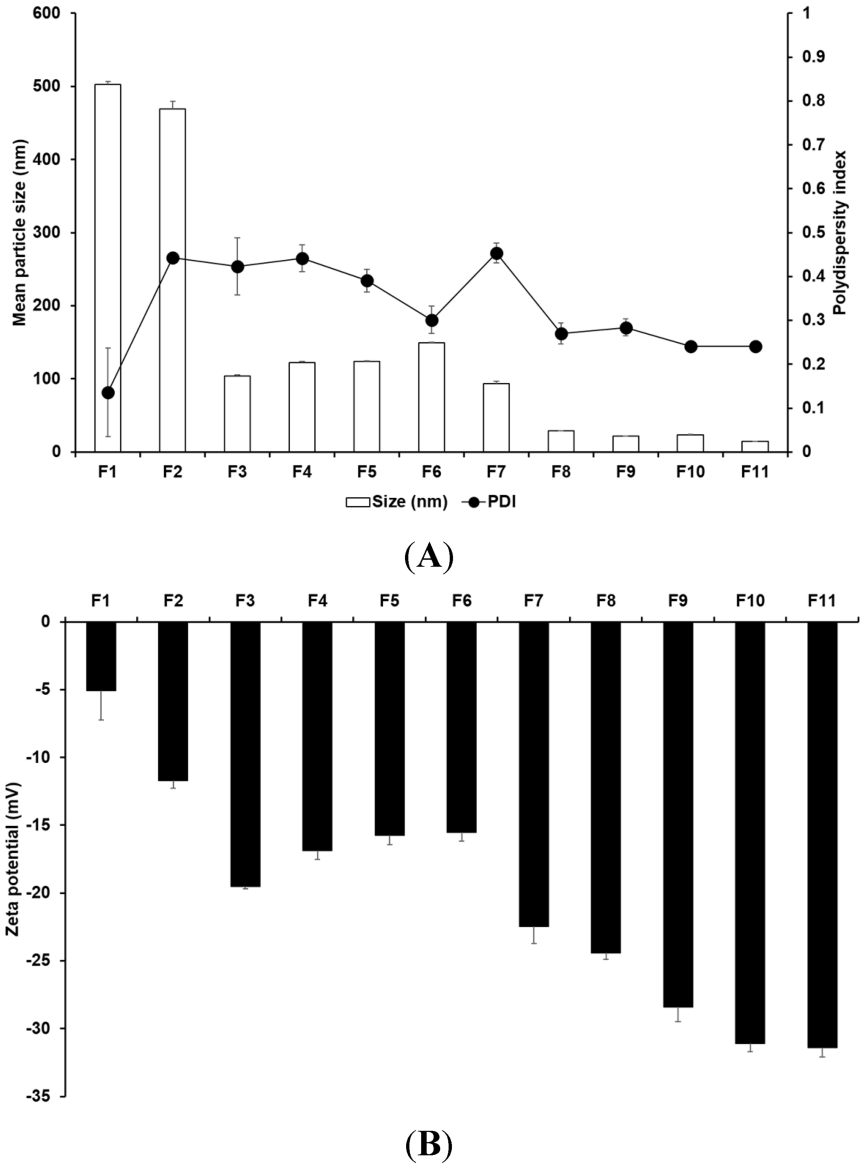

Figure 2. Physicochemical characteristics of the (A) average particle size and PDI and (B) zeta potential for Cur-loaded SLNs prepared using different materials. Results are expressed as the means ± standard deviations of three independent experiments (n = 3). PDI, polydispersity index.

surface, which is an important factor in particle stability.[26,29] Particles with a high zeta potential repel each other, preventing the aggregation of nanoparticles.[30−32] Thus, the storage stability of the particles is higher. In contrast, particles with a low zeta potential facilitate the release of encapsulated drugs. Particle size, PDI, and zeta potential of all the formulations ranged from 14.70 to 502.83 nm, 0.14 to 0.45, and −5.06 to −31.40 mV, respectively (Figure 2). Figure 2 shows the particle size, PDI, and zeta potential of the F1−F3 formulations using different lipids. The formulation using a longer carbon chain lipid resulted in smaller and more stable particles. This suggests that lipids with longer carbon chains may increase surface hydrophobicity.[27,28] Therefore, lipid particles with high surface hydrophobicity have smaller particle sizes in aqueous solutions.[42] The formulations with smaller particle sizes had a high negative charge on the particle surface (Figure 2B). This is because particles with higher surface areas expose the inherent negative charge on the surface.[29,32] In addition, nanoparticles with higher zeta potentials are stable because of the repulsive force among the particles.[31,32]

Among the F3, F4, F5, and F6 formulations formed using different surfactants, F3 had the smallest particle size and highest zeta potential (Figure 2). The particle size and zeta potential of F4 were the second smallest and highest, respectively. This suggests that a surfactant with high hydrophilicity stabilizes the interface between O and W.[29] The hydrophilic−lipophilic balance (HLB) values of PX 188, PX 407, TW 20, and TW 80 were 29, 22, 16.7, and 15, respectively. Consequently, SA and PX 188 were selected as the lipid and surfactant, respectively, to fabricate the SLN.

The effects of the lipid and surfactant concentrations on particle characteristics were determined. An increase in the concentrations of lipids and surfactants decreased the particle size and increased the zeta potential (Figure 2). This suggests that the effect of surfactant concentration on particle size was attributed to the increased hydrophilicity of the formulations.[28] The hydrophilic surfactant contributes to stabilize the interface between O and W, as aforementioned. In this regard, the increased hydrophilicity of the formulations induces that the O phase molecularly dispersing the Cur effectively disperses into

https://doi.org/10.1021/acsomega.2c04407
ACS Omega 2022, 7, 35875−35884

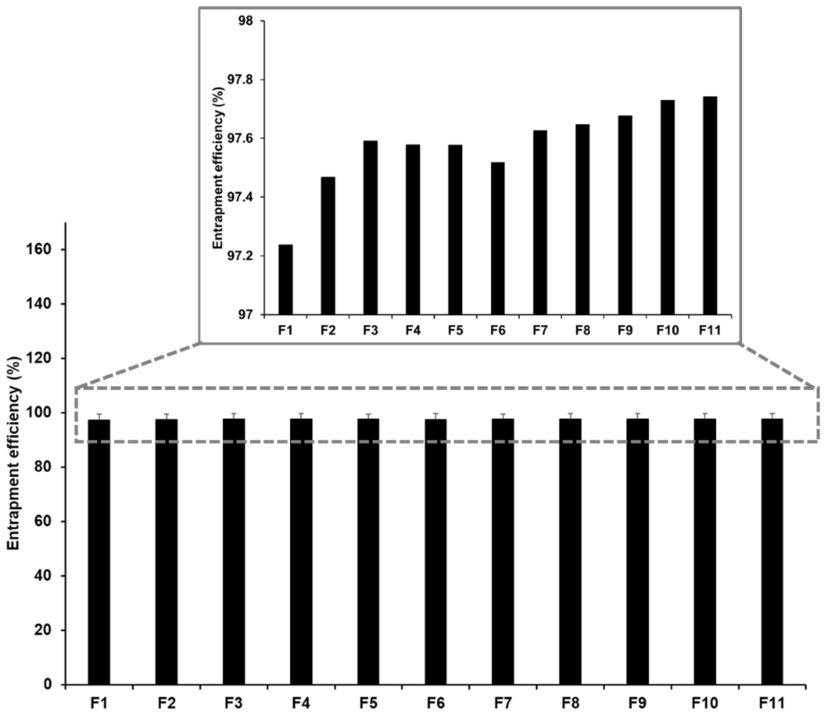

Figure 3. Entrapment efficiency of Cur-loaded SLNs prepared by using different compositions. Results are expressed as the means ± standard deviations of three independent experiments (n = 3). Cur, curcumin.

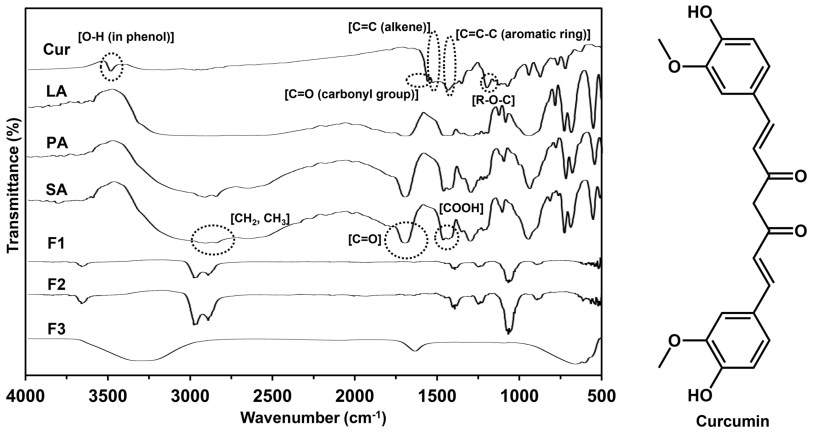

Figure 4. Fourier transform infrared (FTIR) spectroscopy overlay spectra of solid lipid nanoparticles and the structure of Cur. Pure Cur; LA; PA; SA; F1: SLN using LA; F2: SLN using PA; F3: SLN using SA. Cur, curcumin; LA, lauric acid; PA, palmitic acid; SA, stearic acid.

the W phase, which results in the reduced particle size. In addition, the effect of lipid concentration on particle size could be related to the interaction between lipids and Cur.

Determination of Drug-Encapsulation Efficiency (EE). EE is an important parameter in particle formulations because it affects drug stability against the external environment,[2] avoids side effects in the human body that result from exposure to the drug,[32,33] and enables the sustained release of Cur from the formulations.[28] The EE study for Cur-loaded SLN was carried out using the centrifugation method, followed by concentration estimation using the UV−vis method. The EE values ranged from 97.24 to 97.74% (Figure 3). The EE of Cur in the SLNs proportionally increased as the number of lipid carbon chains increased. This was because the log p value of Cur was 3.2, and the lipophilicity of Cur might have a high affinity for lipids with longer carbon chains.[27,28] The higher affinity between the drug and the lipid matrix induces stable encapsulation of the drug in the particle core and shell.[33] Thus, the highest amount of Cur was encapsulated in F3 using SA compared with F1 using LA.

For formulations using different surfactants, the results showed that an increase in the HLB value of the surfactant increased EE. The HLB values for PX 188, PX 407, TW 20, and TW 80 were 29, 22, 16.7, and 15, respectively. This suggests that hydrophilic surfactants stabilize the interface between O and W.[28] In this sense, the more hydrophilic surfactant can stably disperse the O phase, dissolving Cur in the aqueous phase.

Regarding the effect of lipid and surfactant concentrations, the results of EE demonstrated an increase in the amount of lipid and surfactant. This suggests that the lipid and surfactant were utilized as a drug-encapsulated matrix and interface stabilizer to stably disperse the O phase in the aqueous phase, respectively.[26] An increase in the concentration of the

https://doi.org/10.1021/acsomega.2c04407
ACS Omega 2022, 7, 35875−35884

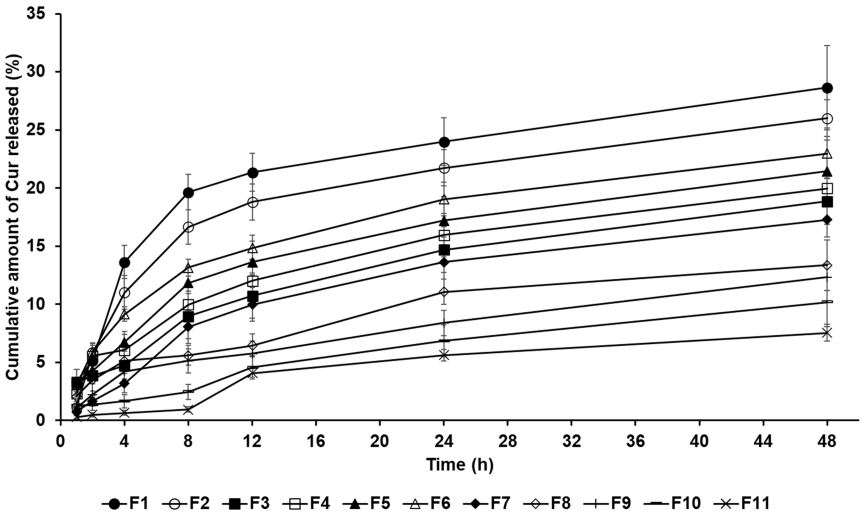

Figure 5. Cumulative percentage release profiles of Cur from SLNs in release medium, as determined using the dialysis bag method. Results are expressed as the means ± standard errors of three independent experiments (n = 3).

ingredients leads to an enhancement of the aforementioned effects. In addition to the effect of the increase in EE, the effect of lipids was stronger than that of surfactants (Figure 3). This might be because the drug loading efficiency was higher in the particle core than that on the particle shell.

FTIR-ATR Spectroscopy. The chemical interactions between Cur and the ingredients of SLN were determined, and the different particle sizes for the formulations were discussed. Figure 4 shows the FTIR spectra of Cur, LA, PA, SA, F1, F2, and F3. The FTIR spectrum of pure Cur showed characteristic peaks at 3014 (O−H stretching in phenol), 1628 (C═O stretching), 1598 (C═C stretching), 1428 and 1508 (C═C—C [aromatic ring]), and 1278 cm^{-1} (R−O−C stretching), as summarized in Table S3. The FTIR spectra of pure lipids (LA, PA, and SA) showed characteristic peaks at 2850 and 2918 (CH_2−CH_3 stretching), 1702 (C═O), and 1465 cm^{-1} (COOH stretching) (Table S4). The FTIR spectra of F1 and F2 demonstrated that in the Cur peaks, the C═C—C stretching peaks shifted to 1406 cm^{-1}, and the O−H, C═O, C═C, and R−O−C stretching peaks were no longer detected, while the CH_2−CH_3 stretching peaks shifted to 2900 and 2971 cm^{-1}, and the C═O and COOH stretching peaks were absent. This suggests that Cur forms a H-bond (hydrogen bond) with lipids (LA and PA) between the carbonyl group (C═O) of Cur and COOH of lipids, phenol (O−H) of Cur and C═O of lipids, and ether (R−O−C) of Cur and COOH of lipids.[1,4] Interactions involving van der Waals forces are also indicated. The possible sites involving van der Waals forces in Cur are C═C (alkene) and C═C—C (aromatic ring), and those in lipids are CH_2−CH_3. The peaks of C═C—C of Cur and CH_2−CH_3 of lipids were shifted in F1 and F2 with the disappearance of C═C of Cur.

The FTIR spectrum of F3 also showed that in the Cur peaks, the C═O stretching peaks shifted to 1636 cm^{-1} and the O−H, C═C, C═C—C, and R−O−C stretching peaks were absent, whereas, in the lipid (SA) peaks, they were no longer detected. This suggests that Cur interacts with SA at each of the two sites via both H-bonds and van der Waals forces. One of the H-bonds is between the phenol (O−H) of Cur and C═O of SA, and the other is between the ether (R−O−C) of Cur and COOH of SA. Regarding van der Waals forces, one of the interactions is between the C═C (alkene) of Cur and CH_2, CH_3 of SA, and the other is between the C═C—C (aromatic ring) of Cur and CH_2, CH_3 of SA.

The chemical structure of Cur is diferuloylmethane, which is a diketone with an aromatic O (*ortho*)-methoxy-phenolic group.[1,4] The structures of LA and PA comprise carbon chains (12 and 16 carbons, respectively) with carboxylic acids, whereas that of SA comprises 18 carbon chains with carboxylic acid.[8−10] This suggests that a lipid with a long carbon chain can bind to a large space of van der Waals forces with Cur, which ranges from aromatic phenol rings to ketones. However, lipids with low carbon chains are not enough to cover the space of van der Waals forces in Cur, ranging from aromatic phenol rings to ketones, which revealed the FTIR spectra of F1 and F2. This may explain the effects of the particle size and EE of Cur-loaded SLNs. In F3 using SA, the small particle size and high EE could be attributed to the neat arrangement of chemical bonds between Cur and SA. In the case of F1 and F2 using LA and PA, the H-bond between the carbonyl group (C═O) of Cur and COOH of lipids, which results from the low carbon chain, disturbs the neat arrangement of the bonds between Cur and lipids (LA and PA). This results in the relatively large particle size and low EE of F1 and F2.

***In Vitro* Cur Release Studies.** The in vitro release profiles of the Cur-loaded SLN were determined using the dialysis membrane method. The results demonstrated that Cur release from Cur-loaded SLNs for 48 h ranged from 7.55 to 28.63% and exhibited a sustained release (Figure 5). Cur-loaded SLNs showed biphasic release profiles, except for F8, F9, F10, and F11, which exhibited a relative burst for 12 h and sustained until 48 h. The first release for 12 h, which was relatively a burst, was attributed to Cur on the surface of the particles that were released rapidly. After that relative burst release, sustained release, which results from Cur in the particle core, was observed until 48 h. The reason for this was the same as that for EE in the EE study. Formulations with high EE can contain a greater amount of drug encapsulated in the particle core than those with low EE, which causes delayed drug release.[28,33] In this regard, a relative burst release for F8, F9, F10, and F11 was not observed.

Regarding the effect of sustained release of used lipids, the formulation using lipids with a longer carbon chain exhibited delayed-release compared to that with a lower carbon chain

https://doi.org/10.1021/acsomega.2c04407
ACS Omega 2022, 7, 35875−35884

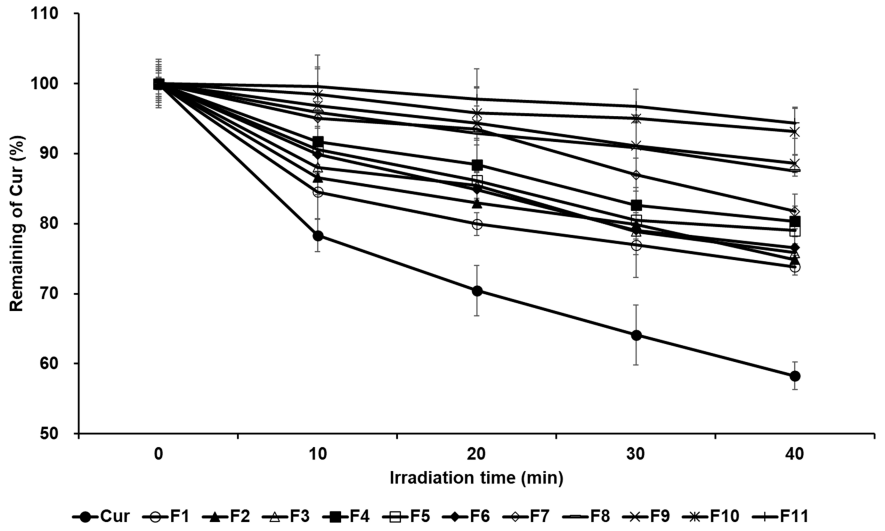

Figure 6. Photostability test using percentage of non-degraded Cur from Cur solution and Cur-loaded SLNs before and after irradiation with LED of 2 J/cm^2 for different time intervals of 0, 10, 20, 30, and 40 min. Results are expressed as means ± standard deviations of three independent experiments (n = 3).

(Figure 5). This suggests that lipids with a long carbon chain can encapsulate Cur in the particle core compared to the shell owing to their lipophilic property.[33] Hence, among F1−F3, which used different lipids, F3 exhibited the lowest release rate. Among F3−F6, which used different surfactants, F3 using PX 188 exhibited delayed release. This suggests that the surfactant with high hydrophilicity effectively stabilized the interface between O and W. Therefore, the formulation with the lowest stability could easily release the drug from the formulation.

Photostability Studies. The photostability of Cur is important for the storage of Cur-loaded SLNs before administration. A moderate dosage should be maintained due to the side effects of the degradation products and the decrease in drug effects. Figure 6 shows the remaining Cur with and without the SLNs. All formulations improved the photostability of Cur (73.82 to 94.39% for 40 min) compared with that of the pure Cur solution (58.26% for 40 min). The Cur photostability of the formulations decreased in the following order after 40 min: F11 > F10 > F9 > F8 > F7 > F4 > F5 > F6 > F3 > F2 > F1 > Cur. This is because SLN can structurally protect encapsulated drugs from the external environment.[32−34] Thus, the photodegradation of Cur was inhibited. Concerning the effects of lipids and surfactants, formulations using lipids with long carbon chains and surfactants with high hydrophilicity tended to have high photostability. This suggests that the encapsulated drug inhibits light exposure, as mentioned above in the EE study.

***In Vitro* Cytotoxicity Using Various Tumor Cells.** The cytotoxic effects of Cur on three cancer cell lines (HeLa, A549, and CT-26) were investigated using the WST assay, as shown in Figure 7 (Tables S5−S7 in the Supporting Information). F1 and F3 were selected as test substances to evaluate the anticancer effects of different lipids and particle sizes. F8 and F10 were also used to determine the effects of the particle size and EE. Each test substance was tested at various concentrations (1, 2.5, 5, and 10 μM) to calculate inhibitory concentration values (IC_{50}). Compared to the pure Cur solution, all formulations exhibited enhanced anticancer effects on HeLa, A549, and CT-26 cells. When treated with 10 μM Cur-loaded SLNs and pure Cur solution, HeLa cells exhibited 21.16−54.10 and 85.43% viability, A549 cells exhibited 23.93−76.67 and 70.94% viability, and CT-26 cells exhibited 44.03−67.32 and 111.19% viability, respectively. The anticancer effect of Cur on A549 cells was the highest among the three cancer cell lines, followed by that on HeLa cells. This suggests that there are different anticancer mechanisms of Cur in HeLa, A549, and CT-26 cells. In HeLa cells, Cur increases both the caspase-3 expression and the activities of caspase-3 and caspase-7, which are directly involved in apoptotic signaling.[43,44] In A549 cells, Cur induces the expression of apoptosis-related proteins, such as caspase-3, caspase-7, and cytochrome C; these increase with a decrease in cyclin-dependent kinase 1 expression, which is involved in cell growth during the G2/M phase of the cell cycle.[45,46] The anticancer effect of Cur on CT-26 cells has been reported to decrease tumor volume by inhibiting cell proliferation.[47]

The order of cytotoxicity of the formulations on all three cell lines was as follows: pure Cur solution < F1 < F3 < F8 < F10. The anticancer effect of F3 using SA was higher than that of F1 using LA. This suggests that the formulation using long-chain lipids satisfies the EPR effect owing to its small particle size and high EE, as mentioned above for the size and EE studies. The cytotoxicity analysis of F3, F8, and F10 demonstrated that F10 exhibited the highest cytotoxic effect, and the IC_{50} values were 1.17 (Hela), 1.03 (A549), and 2.36 μM (CT-26), as summarized in Table 2. The cytotoxicity of F8 was the second highest, and the IC_{50} values were 1.54 (Hela), 1.15 (A549), and 3.03 μM (CT-26), respectively.

Interestingly, the order of the anticancer effect of Cur-loaded SLNs according to the cancer cell lines was as follows: A549 > HeLa > CT-26. This result might be due to the sensitivity of the particle size, such as the EPR effect and cellular uptake, to target cancer cells.[22,24,48] In the size effect studies of Cur applied to A549 cells reported by Choi,[49] Cur-loaded nanoparticles with sizes in the range of 20−80 nm increased the drug concentration in the lung tissue. Additionally, Cur-loaded nanoparticles with a size of 100−150 nm increased the drug concentration in the lungs and cellular uptake.[49,50] In HeLa cells and colon carcinoma cells,[43] nanoparticles with sizes of 100 and 130 nm, respectively, increased the cellular uptake efficiency. Therefore, considering the effects of particle size (EPR effect and cellular uptake) and anticancer mechanisms,

https://doi.org/10.1021/acsomega.2c04407
ACS Omega 2022, 7, 35875−35884

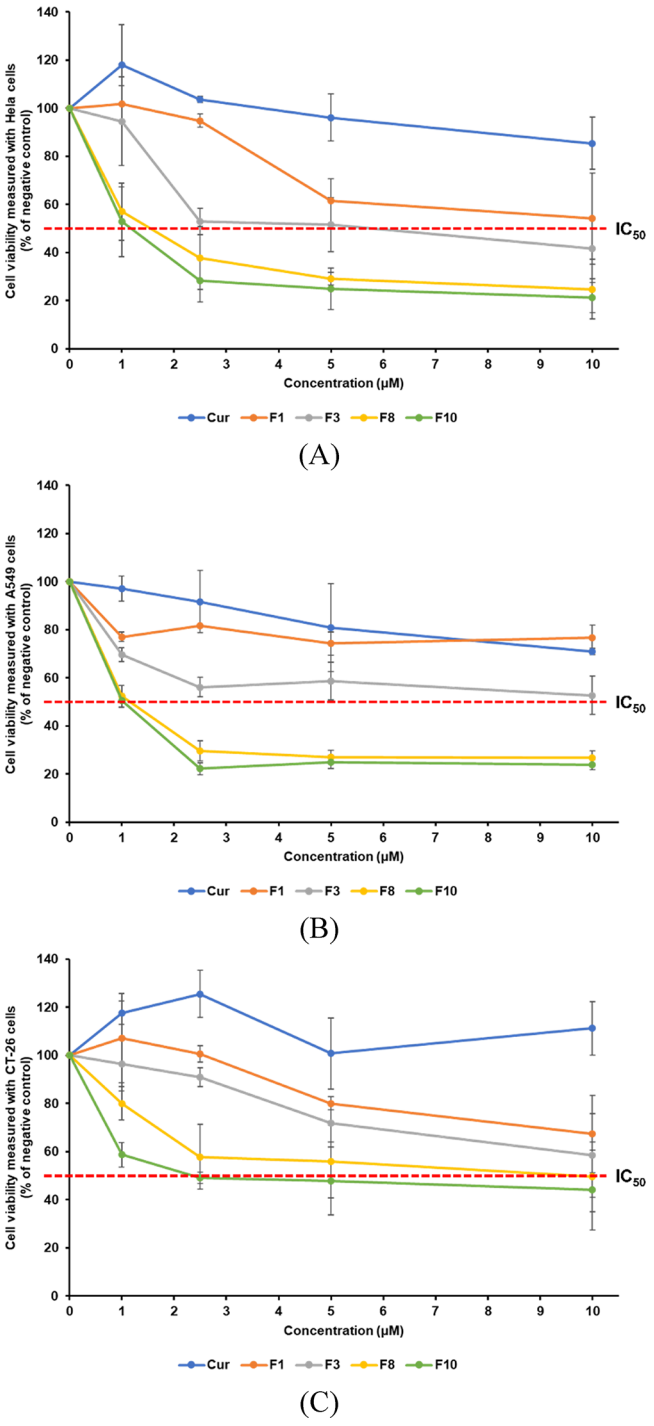

Figure 7. Viability of three cancer cell lines ((A) HeLa, (B) A549, and (C) CT-26) treated with Cur solution, F1, F3, F8, and F10. The cell viability was measured using the WST assay. Results are expressed as means ± standard deviations of three independent experiments (n = 3).

A549 cells may be the most particle size-sensitive tumor cell among the tested cell lines.

CONCLUSIONS

In the present study, we attempted to improve the bioavailability and anticancer effects of Cur. SLNs were prepared by the O/W emulsion method using a probe sonicator. SLNs prepared with LA or PA were large with sizes of 502.83 and 469.53 nm, respectively, whereas those prepared with SA were small, ranging from 14.70 to 149.30 nm. The reason for this is explained by the FTIR results, which confirmed that Cur interacted with lipids via both H-bonding and van der Waals forces. The formulations using SA revealed that an increase in the van der Waals interactions leads to a neat arrangement of the chemical bonds between Cur and SA, which results in relatively small particle size. In this regard, SLNs using SA, which had a relatively high EE, showed delayed drug release profiles with higher photostability than those using LA or PA. Cytotoxicity studies using three cancer cell lines (HeLa, A549, and CT-26) showed that all formulations improved the anticancer effect against these cell lines when compared with pure Cur. Additionally, the cytotoxicity study revealed that the anticancer effect was determined by the particle size and cell line type. Therefore, these results suggest that Cur-loaded SLNs are a promising formulation for anticancer therapy.

Table 2. IC_{50} (μM) Values against HeLa, A549, or CT-26 Cells, Particle Size, and Entrapment Efficiency (EE) of Pure Cur Solution, F1, F3, F8, and F10[a]

	Hela (μM)	A549 (μM)	CT-26 (μM)	particle size (nm)	EE (%)
Cur	>10	>10	>10	N/A	N/A
F1	>10	>10	>10	502.83 ± 3.76	97.24 ± 2.21
F3	5.84	>10	>10	103.90 ± 1.20	97.59 ± 1.97
F8	1.54	1.15	3.03	28.69 ± 0.50	97.65 ± 1.93
F10	1.17	1.03	2.36	23.53 ± 0.22	97.73 ± 1.82

[a]N/A, not applicable.

EXPERIMENTAL SECTION

Materials. Cur and phosphate-buffered saline (PBS) were purchased from Sigma-Aldrich (St. Louis, MO, USA). Lauric acid (LA), palmitic acid (PA), and stearic acid (SA) were supplied by SAMCHUN (Pyeongtaek, Korea). Poloxamer 188 (PX 188) and poloxamer 407 (PX 407) were purchased from BASF (Ludwigshafen, Germany). Tween 20 (TW 20) and Tween 80 (TW 80) were purchased from Dae Jung Co., Ltd. (Busan, Korea). Dulbecco's modified Eagle medium (DMEM) was supplied by WelGENE (Gyeongsan, South Korea). Penicillin−streptomycin solution (100×) and fetal bovine serum (FBS) were purchased from BioWest (Nuaillé, France). The cancer cell lines (HeLa, A549, and CT-26) were purchased from the Korea Cell Line Bank (Seoul, Korea). The Quanti-MAX WST-8 assay kit was purchased from Biomax (Seoul, Korea). High-performance liquid chromatography (HPLC) grade methanol (MeOH) was purchased from Honeywell (Seelze, Germany). All compounds are >95% pure by HPLC analysis.

Preparation of Cur-Loaded SLNs. Cur-loaded SLNs were prepared via sonication using a modified O/W emulsion method. Briefly, the O phase was prepared by dissolving Cur in melted lipid (LA, PA, or SA) at 10 °C above the lipid melting point. The molten O phase was poured into a hot aqueous solution containing surfactants (PX 188, PX 407, TW 20, or TW 80) and homogenized using a polytron homogenizer (PT 3100; Kinematica Instruments, Luzerne, Switzerland) at 1000 rpm, which resulted in an O/W emulsion. SLN were then fabricated by ultrasonication using a probe sonicator (Scientz-IID, Ningbo, China) at 300 W for 15 min with a 5 s pulse-on

https://doi.org/10.1021/acsomega.2c04407
ACS Omega 2022, 7, 35875−35884

period and a 5 s pulse-off period. The effects of different compositions of Cur-loaded SLN were evaluated (Table 1).

Development of Analytical Method for Cur. The concentration of Cur was determined using a UV−vis spectrophotometer (S-3100; Scinco, Seoul, Korea) at ambient temperature. The absorption spectrum of Cur in the wavelength range of 300−800 nm was determined to evaluate its maximum absorption wavelength. MeOH was used as the solvent since the best characteristics of this method were achieved with MeOH. A standard stock solution was prepared by dissolving 2 mg of Cur in 20 mL of MeOH.

The standard stock solution was serially diluted with MeOH to prepare five standard solutions at concentrations of 1−20 ppm. The prepared standard solutions were used to plot a calibration curve (concentration vs absorbance unit) for Cur.

The precision of the analytical method for Cur was determined by performing an assay with six replicate determinations of sample preparation at test concentrations, and the RSD of the assay results was calculated.

The accuracy of the analytical method for Cur was determined by adding a known quantity of the standard to the pre-analyzed sample. To calculate the recovery of Cur, 0, 25, and 100% levels of standard solutions were estimated using the respective UV−vis absorption spectra.

Characterization of Cur-Loaded SLN. *Determination of Nanoparticle Size, PDI, and Zeta Potential.* The particle size PDI of the prepared SLNs was determined at 25 °C by dynamic light scattering using a Zetasizer Nano ZS (Malvern Instruments Ltd., Worcestershire, Malvern, UK). The zeta potential of the SLNs was measured based on the electrophoretic mobility of the particle surface. The samples were diluted 10 times with distilled water (DW) before the measurement. The instrument was equilibrated before each measurement. Each measurement was performed in triplicates.

Determination of Drug-Encapsulation Efficiency (EE). SLN specimens were diluted 10 times to a final volume of 1 mL and then gently vortexed. The suspension was then centrifuged at 1300 rpm for 1 h at 4 °C. The concentration of the free non-encapsulated drug in the supernatant was analyzed using a UV−vis spectrophotometer, as described in the Development of Analytical Method for Cur section. EE was calculated using eq 1.

$$\text{EE}\ (\%) = \frac{\text{total drug amount} - \text{free nonencapsulated drug amount}}{\text{total drug amount}} 100 \quad (1)$$

FTIR Attenuated Total Reflection (ATR) Spectroscopy. Direct information on the chemical interactions between Cur and the ingredients of SLN was obtained using an FTIR-ATR spectrometer (Spectrum Two FT-IR Spectrometer; PerkinElmer, Waltham, MA, USA) equipped with a ZnSe crystal. The spectra across the wavenumber range of 4000−800 cm^{-1} were recorded.

***In Vitro* Cur-Release Studies.** An *in vitro* Cur release study was performed using the dialysis-bag method. Dialysis bags with a molecular weight of 14 kDa (Spectrum Laboratories, Inc., Compton, CA, USA) were soaked in DW for 12 h prior to the experiment. A predetermined amount of each specimen was soaked in dialysis bags, and both ends were sealed using a string. Dialysis bags were immersed in 70 mL vials containing 50 mL of receptor medium (PBS, pH 7.4). The vials were then placed in a shaking incubator (JSSI-100 T; JS Research Inc., Gongju, Korea) and shaken at 100 rpm and 37 ± 0.5 °C. At predetermined time intervals (1, 2, 4, 8, 12, 24, and 48 h), aliquots of 1 mL were withdrawn from the vial, filtered using 0.45 μm membrane filters (SFCA Syringe Filters; Corning Inc., NY, USA), and analyzed immediately using a UV−vis spectrophotometer as described in the Development of Analytical Method for Cur section.

Photostability Studies. The photostability of Cur in SLNs was determined according to the modified method described by Lima et al. and compared with that of Cur in a 0.1% MeOH solution.[40] The photostability of Cur was monitored by recording its absorption spectrum at 425 nm. Briefly, 20 mL of Cur- or Cur-loaded SLNs in a 0.1% MeOH solution (4 ppm) was irradiated (2 J/cm^2) with LED for different time intervals (0, 10, 20, 30, and 40 min). Cur was then extracted from the formulations by adding 1 mL of hexane to dissolve the lipids, followed by vortexing. A 0.1% MeOH layer containing the extracted Cur was filtered through 0.22 μm filters and analyzed using the UV−vis spectrophotometer as described in the Development of Analytical Method for Cur section.

Determination of *In Vitro* Cytotoxicity. *Cytotoxicity Study Using Various Tumor Cells.* The anticancer efficacy of Cur was investigated based on its cytotoxic effects on three cell lines (HeLa from human cervical carcinoma, A549 from human lung carcinoma, and CT-26 from mouse colon carcinoma). Each cell line was seeded into 48-well plates at a density of 2×10^4 cells/well, and the number of cells was calculated using the hemocytometer method. Prior to each experiment, the cells were incubated for 24 h at 37 ± 0.5 °C in a humidified atmosphere with 5% CO_2. Various concentrations (1, 2.5, 5, or 10 μM) of each sample were then added to each well. After 24 h, the cells were rinsed with sterile PBS, and 200 μL/well of the growth medium was added. The treated cells were incubated for 24 h at 37 ± 0.5 °C and 5% CO_2 for the WST reduction experiment, as described in the Viability of Cancer Cells section.

Viability of Cancer Cells. Cytotoxicity was determined by measuring the dehydrogenase activity of viable keratinocytes 24 h post-incubation. The dehydrogenase activity was determined after the incorporation of WST, as described previously.[41] Each cell line was treated with 100 μL/well of a 10% WST solution for 1 h. The WST concentration was measured by determining the optical density (OD) at 450 nm using a microplate reader.

Each experiment was conducted in at least three wells of the plate. After subtracting the blank OD from all raw data, the mean OD values ± standard deviations (SDs) were calculated using three measurements per test substance, and the percentage of cell viability relative to that of the negative control was calculated using eq 2. The viability of the negative control was set to 100%.

$$\text{viability}\ (\%) = \frac{\text{mean OD}_{\text{treated}}}{\text{mean OD}_{\text{control}}} \times 100 \quad (2)$$

Statistical Analysis. Three independent experiments were performed for all analyses. The presented data (mean ± SDs) were compared using one-way analysis of variance and Student's *t*-test. Statistical significance was set at $P < 0.05$.

https://doi.org/10.1021/acsomega.2c04407
ACS Omega 2022, 7, 35875−35884

■ ASSOCIATED CONTENT

Supporting Information

The Supporting Information is available free of charge at https://pubs.acs.org/doi/10.1021/acsomega.2c04407.

Linearity data of Cur standard stock solution; precision data; accuracy data; summarized FTIR peaks; in vitro photoirritation studies (PDF)

■ AUTHOR INFORMATION

Corresponding Authors

Sooho Yeo − *Center for Nano Manufacturing and Department of Nanoscience and Engineering, Inje University, Gimhae 50834, South Korea;* orcid.org/0000-0002-6046-3168; Email: sooho32@inje.ac.kr

Il Yoon − *Center for Nano Manufacturing and Department of Nanoscience and Engineering, Inje University, Gimhae 50834, South Korea*; Email: yoonil71@inje.ac.kr

Woo Kyoung Lee − *Center for Nano Manufacturing and Department of Nanoscience and Engineering, Inje University, Gimhae 50834, South Korea*; Email: wlee@inje.ac.kr

Authors

Min Je Kim − *Center for Nano Manufacturing and Department of Nanoscience and Engineering, Inje University, Gimhae 50834, South Korea*

Young Key Shim − *Center for Nano Manufacturing and Department of Nanoscience and Engineering, Inje University, Gimhae 50834, South Korea*

Complete contact information is available at: https://pubs.acs.org/10.1021/acsomega.2c04407

Author Contributions

Conceptualization was done by S.Y., Y.K.S., I.Y., and W.K.L.; methodology was done by S.Y. and M.J.K.; resource gathering was done by I.Y. and W.K.L.; writing and original draft preparation were done by S.Y. and I.Y.; funding acquisition was done by I.Y. and W.K.L.; and supervision was done by W.K.L. All authors have read and agreed to the published version of the manuscript.

Notes

The authors declare no competing financial interest.

■ ACKNOWLEDGMENTS

This research was supported by the BK21 FOUR (Fostering Outstanding Universities for Research, No.5199991614715), the National Research Foundation of Korea (NRF) grant, the Basic Science Research Program through the National Research Foundation of Korea (NRF) funded by the Ministry of Education (MOE, Korea, NRF-2020R1I1A1A01060632), and the Korean government (MSIT) (NRF-2020R1F1A1070571).

■ ABBREVIATIONS USED

Cur, curcumin; SLN, solid lipid nanoparticle; FTIR, Fourier transform infrared spectroscopy; EPR, enhanced permeation and retention; BCS, biopharmaceutical classification system; LA, lauric acid; PA, palmitic acid; SA, stearic acid; EE, encapsulation efficiency; HPLC, high-performance liquid chromatography; MeOH, methanol; O/W, oil-in-water phase

■ REFERENCES

(1) Lee, W.-H.; Loo, C.-Y.; Bebawy, M.; Luk, F.; Mason, R.; Rohanizadeh, R. Curcumin and its derivatives: their application in neuropharmacology and neuroscience in the 21st century. *Curr. Neuropharmacol.* **2013**, *11*, 338−378.

(2) Mahmud, M.; Piwoni, A.; Filiczak, N.; Janicka, M.; Gubernator, J. Long-circulating curcumin-loaded liposome formulations with high incorporation efficiency, stability and anticancer activity towards pancreatic adenocarcinoma cell lines in vitro. *PLoS One* **2016**, *11*, No. e0167787.

(3) Shahani, K.; Swaminathan, S. K.; Freeman, D.; Blum, A.; Ma, L.; Panyam, J. Injectable sustained release microparticles of curcumin: a new concept for cancer chemoprevention. *Cancer Res.* **2010**, *70*, 4443−4452.

(4) Jankun, J.; Wyganowska-Świątkowska, M.; Dettlaff, K.; Jelińska, A.; Surdacka, A.; Wątróbska-Świetlikowska, D.; Skrzypczak-Jankun, E. Determining whether curcumin degradation/condensation is actually bioactivation (Review). *Int. J. Mol. Med.* **2016**, *37*, 1151−1158.

(5) Pescosolido, N.; Giannotti, R.; Plateroti, A. M.; Pascarella, A.; Nebbioso, M. Curcumin: therapeutical potential in ophthalmology. *Planta Med.* **2014**, *80*, 249−254.

(6) Chetoni, P.; Burgalassi, S.; Monti, D.; Tampucci, S.; Tullio, V.; Cuffini, A. M.; Muntoni, E.; Spagnolo, R.; Zara, G. P.; Cavalli, R. Solid lipid nanoparticles as promising tool for intraocular tobramycin delivery: Pharmacokinetic studies on rabbits. *Eur. J. Pharm. Biopharm.* **2016**, *109*, 214−223.

(7) Yadav, M.; Schiavone, N.; Guzman-Aranguez, A.; Giansanti, F.; Papucci, L.; Perez de Lara, M. J.; Singh, M.; Kaur, I. P. Atorvastatin-loaded solid lipid nanoparticles as eye drops: Proposed treatment option for age-related macular degeneration (AMD). *Drug Delivery Transl. Res.* **2020**, *10*, 919−944.

(8) Huang, S.; He, J.; Cao, L.; Lin, H.; Zhang, W.; Zhong, Q. Improved physicochemical properties of curcumin-loaded solid lipid nanoparticles stabilized by sodium caseinate-lactose Maillard conjugate. *J. Agric. Food Chem.* **2020**, *68*, 7072−7081.

(9) Kumar, P. S.; Punniamurthy, N. Formulation development and characterization of curcumin loaded solid lipid nanoparticles for improved aqueous solubility and bioavailability. *J. Pharm. Innovation* **2017**, *6*, 7.

(10) Teixeira, A. C. T.; Fernandes, A. C.; Garcia, A. R.; Ilharco, L. M.; Brogueira, P.; da Silva, A. M. P. S. G. Microdomains in mixed monolayers of oleanolic and stearic acids: thermodynamic study and BAM observation at the air−water interface and AFM and FTIR analysis of LB monolayers. *Chem. Phys. Lipids* **2007**, *149*, 1−13.

(11) Jamwal, R. Bioavailable curcumin formulations: A review of pharmacokinetic studies in healthy volunteers. *J. Integr. Med.* **2018**, *16*, 367−374.

(12) Ravindranath, V.; Chandrasekhara, N. Absorption and tissue distribution of curcumin in rats. *Toxicology* **1980**, *16*, 259−265.

(13) Anand, P.; Kunnumakkara, A. B.; Newman, R. A.; Aggarwal, B. B. Bioavailability of curcumin: problems and promises. *Mol. Pharmaceutics* **2007**, *4*, 807−818.

(14) Muangnoi, C.; Jithavech, P.; Ratnatilaka Na Bhuket, P.; Supasena, W.; Wichitnithad, W.; Towiwat, P.; Niwattisaiwong, N.; Haworth, I. S.; Rojsitthisak, P. A curcumin-diglutaric acid conjugated prodrug with improved water solubility and antinociceptive properties compared to curcumin. *Biosci., Biotechnol., Biochem.* **2018**, *82*, 1301−1308.

(15) Manju, S.; Sreenivasan, K. Conjugation of curcumin onto hyaluronic acid enhances its aqueous solubility and stability. *J. Colloid Interface Sci.* **2011**, *359*, 318−325.

(16) Li, L.; Braiteh, F. S.; Kurzrock, R. Liposome-encapsulated curcumin: in vitro and in vivo effects on proliferation, apoptosis, signaling, and angiogenesis. *Cancer* **2005**, *104*, 1322−1331.

(17) Salmazi, R.; Calixto, G.; Bernegossi, J.; dos Santos Ramos, M. A.; Bauab, T. M.; Chorilli, M. A curcumin-loaded liquid crystal precursor mucoadhesive system for the treatment of vaginal candidiasis. *Int. J. Nanomed.* **2015**, *10*, 4815.

(18) Sari, T. P.; Mann, B.; Kumar, R.; Singh, R. R. B.; Sharma, R.; Bhardwaj, M.; Athira, S. Preparation and characterization of nanoemulsion encapsulating curcumin. *Food Hydrocolloids* **2015**, *43*, 540−546.
(19) Liu, A.; Lou, H.; Zhao, L.; Fan, P. Validated LC/MS/MS assay for curcumin and tetrahydrocurcumin in rat plasma and application to pharmacokinetic study of phospholipid complex of curcumin. *J. Pharm. Biomed. Anal.* **2006**, *40*, 720−727.
(20) Zhou, S.; Shang, Q.; Wang, N.; Li, Q.; Song, A.; Luan, Y. Rational design of a minimalist nanoplatform to maximize immunotherapeutic efficacy: Four birds with one stone. *J. Controlled Release* **2020**, *328*, 617−630.
(21) Zhang, M.; Qin, X.; Zhao, Z.; Du, Q.; Li, Q.; Jiang, Y.; Luan, Y. A self-amplifying nanodrug to manipulate the Janus-faced nature of ferroptosis for tumor therapy. *Nanoscale Horiz.* **2022**, *7*, 198−210.
(22) Alavi, M.; Hamidi, M. Passive and active targeting in cancer therapy by liposomes and lipid nanoparticles. *Drug Metab. Pers. Ther.* **2019**, *34*, DOI: 10.1515/dmpt-2018-0032.
(23) Gu, W.; Meng, F.; Haag, R.; Zhong, Z. Actively targeted nanomedicines for precision cancer therapy: Concept, construction, challenges and clinical translation. *J. Controlled Release* **2021**, *329*, 676−695.
(24) Yahya, E. B.; Alqadhi, A. M. Recent trends in cancer therapy: a review on the current state of gene delivery. *Life Sci.* **2021**, *269*, No. 119087.
(25) Nahar, P. P.; Slitt, A. L.; Seeram, N. P. Anti-inflammatory effects of novel standardized solid lipid curcumin formulations. *J. Med. Food* **2015**, *18*, 786−792.
(26) Araya-Sibaja, A. M.; Salazar-López, N. J.; Romero, K. W.; Vega-Baudrit, J. R.; Domínguez-Avila, J. A.; Contreras, C. A. V.; Robles-Zepeda, R. E.; Navarro-Hoyos, M.; González-Aguilar, G. A. Use of nanosystems to improve the anticancer effects of curcumin. *Beilstein J. Nanotechnol.* **2021**, *12*, 1047−1062.
(27) Pashkovskaya, A. A.; Vazdar, M.; Zimmermann, L.; Jovanovic, O.; Pohl, P.; Pohl, E. E. Mechanism of long-chain free fatty acid protonation at the membrane-water interface. *Biophys. J.* **2018**, *114*, 2142−2151.
(28) Müller, R. H.; Mäder, K.; Gohla, S. Solid lipid nanoparticles (SLN) for controlled drug delivery−a review of the state of the art. *Eur. J. Pharm. Biopharm.* **2000**, *50*, 161−177.
(29) Tiyaboonchai, W.; Tungpradit, W.; Plianbangchang, P. Formulation and characterization of curcuminoids loaded solid lipid nanoparticles. *Int. J. Pharm.* **2007**, *337*, 299−306.
(30) Sharifi, S.; Fathi, N.; Memar, M. Y.; Hosseiniyan Khatibi, S. M.; Khalilov, R.; Negahdari, R.; Zununi Vahed, S.; Maleki Dizaj, S. Antimicrobial activity of curcumin nanoformulations: New trends and future perspectives. *Phytother. Res.* **2020**, *34*, 1926−1946.
(31) Youssef, T.; Fadel, M.; Fahmy, R.; Kassab, K. Evaluation of hypericin-loaded solid lipid nanoparticles: physicochemical properties, photostability and phototoxicity. *Pharm. Dev. Technol.* **2012**, *17*, 177−186.
(32) Radomska-Soukharev, A. Stability of lipid excipients in solid lipid nanoparticles. *Adv. Drug Delivery Rev.* **2007**, *59*, 411−418.
(33) Kuklenyik, Z.; Jones, J. I.; Gardner, M. S.; Schieltz, D. M.; Parks, B. A.; Toth, C. A.; Rees, J. C.; Andrews, M. L.; Carter, K.; Lehtikoski, A. K.; McWilliams, L. G.; Williamson, Y. M.; Bierbaum, K. P.; Pirkle, J. L.; Barr, J. R. Core lipid, surface lipid and apolipoprotein composition analysis of lipoprotein particles as a function of particle size in one workflow integrating asymmetric flow field-flow fractionation and liquid chromatography-tandem mass spectrometry. *PLoS One* **2018**, *13*, No. e0194797.
(34) Dodangeh, M.; Tang, R.-C.; Gharanjig, K. Improving the photostability of curcumin using functional star-shaped polyamidoamine dendrimer: Application on PET. *Mater. Today Commun.* **2019**, *21*, No. 100620.
(35) Makwana, V.; Jain, R.; Patel, K.; Nivsarkar, M.; Joshi, A. Solid lipid nanoparticles (SLN) of Efavirenz as lymph targeting drug delivery system: Elucidation of mechanism of uptake using chylomicron flow blocking approach. *Int. J. Pharm.* **2015**, *495*, 439−446.
(36) Yasir, M.; Gaur, P. K.; Puri, D.; Shehkar, P.; Kumar, S. S. Solid lipid nanoparticles approach for lymphatic targeting through intraduodenal delivery of quetiapine fumarate. *Curr. Drug Delivery* **2018**, *15*, 818−828.
(37) Graverini, G.; Piazzini, V.; Landucci, E.; Pantano, D.; Nardiello, P.; Casamenti, F.; Pellegrini-Giampietro, D. E.; Bilia, A. R.; Bergonzi, M. C. Solid lipid nanoparticles for delivery of andrographolide across the blood-brain barrier: in vitro and in vivo evaluation. *Colloids Surf., B* **2018**, *161*, 302−313.
(38) Ghasemiyeh, P.; Mohammadi-Samani, S. Solid lipid nanoparticles and nanostructured lipid carriers as novel drug delivery systems: applications, advantages and disadvantages. *Res. Pharm. Sci.* **2018**, *13*, 288.
(39) Rhea, E. M.; Banks, W. A. Role of the blood-brain barrier in central nervous system insulin resistance. *Front. Neurosci.* **2019**, *13*, 521.
(40) Lima, A. M.; Dal Pizzol, C.; Monteiro, F. B.; Creczynski-Pasa, T. B.; Andrade, G. P.; Ribeiro, A. O.; Perussi, J. R. Hypericin encapsulated in solid lipid nanoparticles: phototoxicity and photodynamic efficiency. *J. Photochem. Photobiol., B* **2013**, *125*, 146−154.
(41) Alépée, N.; Tornier, C.; Robert, C.; Amsellem, C.; Roux, M.-H.; Doucet, O.; Pachot, J.; Méloni, M.; de Fraissinette, A. d. B. A catch-up validation study on reconstructed human epidermis (SkinEthic™ RHE) for full replacement of the Draize skin irritation test. *Toxicol. In Vitro* **2010**, *24*, 257−266.
(42) Péroval, C.; Debeaufort, F.; Despré, D.; Voilley, A. Edible arabinoxylan-based films. 1. Effects of lipid type on water vapor permeability, film structure, and other physical characteristics. *J. Agric. Food Chem.* **2002**, *50*, 3977−3983.
(43) Zhang, H.; Zhang, Y.; Chen, Y.; Zhang, Y.; Wang, Y.; Zhang, Y.; Song, L.; Jiang, B.; Su, G.; Li, Y.; Hou, Z. Glutathione-responsive self-delivery nanoparticles assembled by curcumin dimer for enhanced intracellular drug delivery. *Int. J. Pharm.* **2018**, *549*, 230−238.
(44) Ratul Kumar, D.; Naresh, K.; Utpal, B. Encapsulation of curcumin in alginate-chitosan-pluronic composite nanoparticles for delivery to cancer cells. *Nanomed.: Nanotechnol., Biol. Med.* **2010**, *6*, 153−160.
(45) Gaikwad, D.; Shewale, R.; Patil, V.; Mali, D.; Gaikwad, U.; Jadhav, N. Enhancement in in vitro anti-angiogenesis activity and cytotoxicity in lung cancer cell by pectin-PVP based curcumin particulates. *Int. J. Biol. Macromol.* **2017**, *104*, 656−664.
(46) Chang, H.-B.; Chen, B.-H. Inhibition of lung cancer cells A549 and H460 by curcuminoid extracts and nanoemulsions prepared from Curcuma longa Linnaeus. *Int. J. Nanomed.* **2015**, *10*, 5059.
(47) Sesarman, A.; Tefas, L.; Sylvester, B.; Licarete, E.; Rauca, V.; Luput, L.; Patras, L.; Banciu, M.; Porfire, A. Anti-angiogenic and anti-inflammatory effects of long-circulating liposomes co-encapsulating curcumin and doxorubicin on C26 murine colon cancer cells. *Pharmacol. Rep.* **2018**, *70*, 331−339.
(48) Jafari, Z.; Bigham, A.; Sadeghi, S.; Dehdashti, S. M.; Rabiee, N.; Abedivash, A.; Bagherzadeh, M.; Nasseri, B.; Karimi-Maleh, H.; Sharifi, E.; Varma, R. S.; Makvandi, P. Nanotechnology-Abetted astaxanthin formulations in multimodel therapeutic and biomedical applications. *J. Med. Chem.* **2022**, *65*, 2−36.
(49) Choi, J.-S. Development of surface curcumin nanoparticles modified with biological macromolecules for anti-tumor effects. *Int. J. Biol. Macromol.* **2016**, *92*, 850−859.
(50) Tian, C.; Guo, J.; Miao, Y.; Zheng, S.; Sun, B.; Sun, M.; Ye, Q.; Liu, W.; Zhou, S.; Kamei, K.; He, Z.; Sun, J. Triglyceride-Mimetic Structure-Gated Prodrug Nanoparticles for Smart Cancer Therapy. *J. Med. Chem.* **2021**, *64*, 15936−15948.

https://doi.org/10.1021/acsomega.2c04407
ACS Omega 2022, 7, 35875−35884